Numerical investigations on the secondary flow characteristics of a turbine stator cascade

Abhilash.R, S.Anil Lal
Department of Mechanical Engineering
College of Engineering Trivandrum
abhilashr@cet.ac.in
anillal@cet.ac.in

***Abstract*—This paper reports the characteristics of flow in axial turbine stator cascade predicted numerically using an open source CFD tool, OpenFOAM. The main objective of this work is to understand the secondary flows such as maximum secondary flow velocity, secondary kinetic energy, its location etc.Understanding the vortices and identifying regions with maximun secondary kinetic energy will help to device methods to reduce or eliminate the secondary flow vortices and there by increase the efficiency of the turbine. An effort is also made to understand the effect of variation of span in the intensity of secondary flow structures. The cross section of the blade is taken as NACA 0012 and the span considered as straight.**

I. Introduction

Flow in turbomachines is an important area of contemporary research. Primary flow is the flow responsible for production of energy in a turbomachine. The flow occurring in a direction transverse to that of the primary flow is the secondary flow. The secondary flows are undesirable as they reduce the energy available for torque generation and result in low efficiency. The understanding of the origin and nature of the secondary flows is very important as it will help in devising methods to reduce them. The reduction in the intensity of secondary flows will increase the mechanical energy produced per unit of fuel consumed. Reducing the combustion has a direct impact on reducing the environmental degradation.A turbine stage consists of a stator and a rotor blade. The figure 1 shows the schematic diagram of a turbine stage.

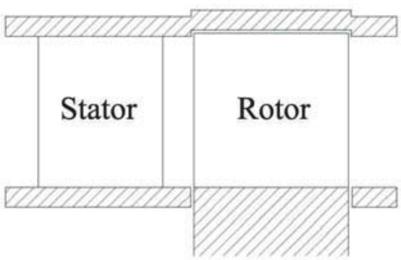

Fig. 1. Schematic diagram of a turbine stage

In the present study the three dimensional flow characteristics of a stator cascade, without clearance gap at the tip of the blade is analysed. The cross section of the blade is taken as NACA 0012 and the span considered as straight.

II. Literature review

Secondary flow structures, their interaction and methods for reduction is an integral part of turbomachinery research. The research in this field dates back to 1950s and is still an active domain. Work in the early period was predominantly experimental and recently it contains numerical as well. The structures in secondary flow can be classified as

1) Horse shoe vortex
2) Passage vortex
3) Corner vortices

The fluid near the centre of the span is decelerated more than the fluid near the hub and the tip walls. This will set up a static pressure gradient along the span causing the higher velocity fluid to turn towards the end-wall. Due to the boundary layer fluid elements form a reverse recirculating flow, called the horse shoe vortex just before the leading edge. The upstream boundary layer rolled-up in the recirculating zone flows past the leading edge and is transported downstream in two legs, namely pressure-side and suction-side leg of the horse-shoe vortex. Momentum equation in the cross stream direction is given by

$$\frac{\rho v^2}{S} = \frac{\partial p}{\partial z}$$

where ρ is the density, v is the velocity, S is the stream line curvature radius, p is the pressure and z is the normal coordinate. With a decrease of the velocity in the boundary layer, a reduction of the streamline curvature radius in the boundary layer flow is required in order to balance the cross passage (pitch-wise)pressure gradient formed in the channel. As a result of this, the boundary layer flow is turned more compared to the main flow in the blade-to-blade channel, leading to a flow from the pressure to suction surface in the end-wall boundary layer. A compensating return flow must then occur at a certain distance from the end-wall, giving rise to the recirculating flow. This recirculating flow combines with the pressure side leg of the horse shoe vortex to form the passage vortex which is the predominant structure. The corner vortices are formed due to the induction of the main flow structures such as pressure and suction side leg of horse shoe vortex and the passage vortex.The induced vortices are leading edge corner vortices, suction side and pressure side corner vortices and wall vortex. The corner vortices are formed at the corner between the blade / vane and the end-wall. A number of models that describe the formation and interaction of the vortices have been proposed by Langston [1], Sharma and Butler [2], Sieverding [3], Wang et al. [4]. The horse shoe vortex formation around a cylinder was studied in detail by Eckerle et al. [5]. The measurements were taken at the symmetric plane and also for planes at various angles to understand the flow separation and location of saddle point. The saddle point is the point at which the incoming and reverse flow velocity vector meet. An important work to investigate a method to reduce the intensity of horse shoe vortex at leading edge by the application of a fillet is done by Zess and Thole [9], they have demonstrated the importance of secondary kinetic energy (SKE) as the optimisation parameter in identifying and reducing the horse shoe vortex and thereby increasing turbine efficiency. A detailed description of the optimisation parameters used in the study of turbomachines is given in [6]. The paper highlights the importance of optimisation parameters such as minimisation of SKE in devising methods for reducing the secondary flows.

III. Validation

The open source code, OpenFOAM is to be validated to understand its capability to predict the compressible flow characteristics and vortex capture capabilities. For this the problem of laminar flow over an isolated NACA 0012 aerofoil previously investigated by a number of researchers is solved. An important feature of this flow is the presence of trailing edge vortice and separation at 82.5 % of span as given by Swanson et al. [7] and [8]. A two dimensional isolated aerofoil with a chord of unity and flow domain extending a chord in each direction is considered. The flow Reynolds number is 5000 and free stream Mach number is taken as 0.5. The figure 2 shows the laminar separation bubble obtained from the analysis . The figure 3 shows the skin friction coefficient along the span obtained in the present study. The point of separation is also obtained at 82.5 % of the span

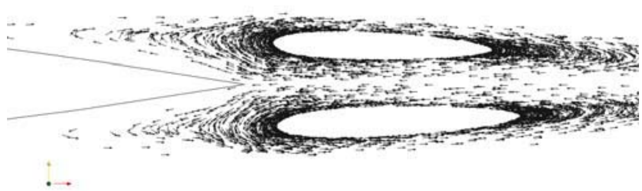

Fig. 2. Laminar separation bubble

IV. Governing Equation

The Reynolds averaged Navier Stokes equation is solved using Launder Sharma K-ϵ turbulence model. The governing equations for k and ϵ are shown below.

$$\frac{\partial}{\partial t}(\rho k)+\frac{\partial}{\partial x_j}\left[\rho k u_j-\left(\mu+\frac{\mu_t}{\sigma_k}\right)\frac{\partial k}{\partial x_j}\right]=P-\rho\epsilon-\rho D \quad (1)$$

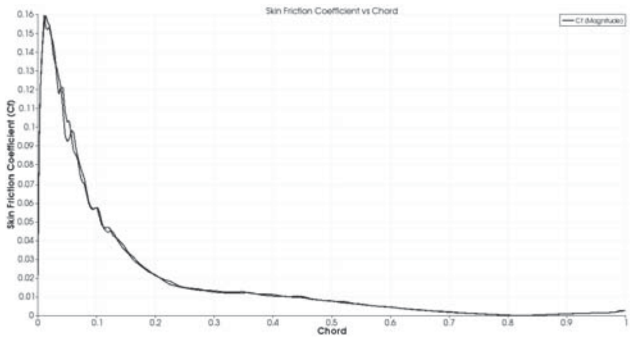

Fig. 3. Skin friction coefficient along span

$$\frac{\partial}{\partial t}(\rho\epsilon)+\frac{\partial}{\partial x_j}\left[\rho\epsilon u_j-\left(\mu+\frac{\mu_t}{\sigma_\epsilon}\right)\frac{\partial \epsilon}{\partial x_j}\right] = \left(C_{\epsilon_1} f_1 P - C_{\epsilon_2} f_2 \rho\epsilon\right)\frac{\epsilon}{k}+\rho E \quad (2)$$

$$\mu_t = C_\mu f_\mu \rho \frac{k^2}{\epsilon} \quad (3)$$

$$P = \tau_{ij}^{turb}\frac{\partial u_i}{\partial x_j} \quad (4)$$

ϵ_1, C_{ϵ_2}, C_μ, σ_k and σ_ϵ are model constants. The damping functions f_μ, f_1 and f_2 and the extra source terms $D$and E are only active close to solid walls and makes it possible to solve k and ϵ down to the viscous sublayer

V. Model and Meshing

The modeling and meshing was done using ICEMCFD. A two dimensional cascade was modeled in ICEMCFD, meshed using block mesh which gives structured mesh. The physical model obtained in computer is as shown in figure 4. The meshed model was exported to OpenFOAM and extruded for the spanwise direction. Boundary layer grid is given in the spanwise direction near the wall. The NACA 0012 blade has a span of 1m. The flow domain extends 0.5 m upstream of the leading edge and 1m downstream of the trailing edge. A distance equal to half of the chord was given above and below the aerofoil to fix the periodic boundaries. The mesh developed for the study is shown in figure 5. A boundary layer grid is given over the aerofoil and a fine mesh is also given at the region where shock is expected.

VI. Boundary conditions

The stagnation pressure at inlet is taken as 138710 N/m^2 and the static pressure at exit is taken as $100000 N/m^2$. These values correspond to an isentropic Mach number of 0.7 at exit. The temperature of free stream is taken as 288.15 K at inlet. The turbulence model used is Launder-Sharma k-ϵ model and the values of α_t, μ_t, k and ϵ are given accordingly. A periodic boundary condition is given in the pitchwise direction. The bottom surface (spanwise direction) is given wall boundary conditions and the top surface is given symmetry boundary condition. A no slip condition for velocity and zero normal pressure gradient are used as boundary condition over the solid surface of the aerofoil.

Fig. 4. Three dimensional model and flow domain

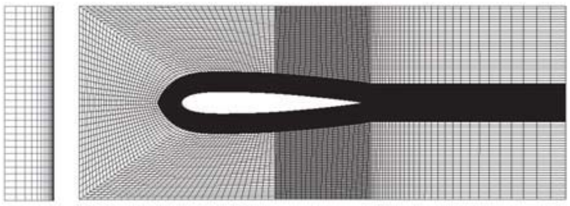

Fig. 5. The meshed model with BL grids

VII. Results and Discussion

The analysis on NACA 0012 stator cascade is conducted.

A. Case 1 : Span =0.3 chord

The chord of the aerofoil is fixed as 1.0 m and a span of 0.3 times the chord is considerd for the first case. The figure 6 shows the velocity plot at the upstream side of the leading edge along the meridonial span plane. The enlarged view of the vectors close to the aerofoil and over the surface of the bottom endwall shows recirculation as also shown in the figure.

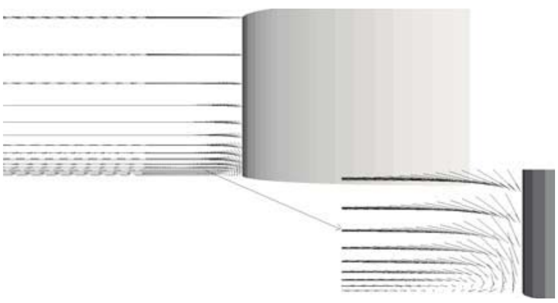

Fig. 6. Recirculation flow upstram of the blade and over the surface of bottom endwall

B. Case 2 : Variation of Secondary flow with span

To understand the variation in secondary flow with span Different values of span have been analysed by keeping the chord at a constant value of 1.0 m and at a free stream Mach number of 0.8. The values of span to chord ratio used for the analysis are 0.2, 0.3, 0.4, and 1.0. Since the flow is set on the x - direction the magnitude of the secondary velocity at any point is $\sqrt{V_y^2 + V_z^2}$, where $V_y$and V_z are the components of velocity along the y and z direction. The Secondary Kinetic Energy per volume (SKE) is calculated as $SKE = \frac{1}{2}\rho(V_y^2 + V_z^2)$

The variation in the secondary flow with span is given in figure 7. The x axis shows the span height as percentage of chord length and y -axis shows the secondary velocity in m/s.

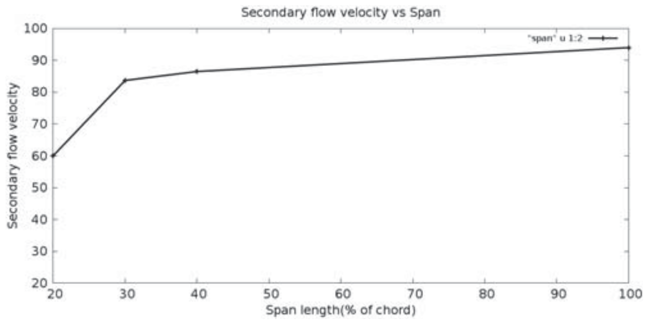

Fig. 7. The variation of maximum value of secondary velocity with variation of span

The variation of secondary flow velocity in d direction transverse to the direction of flow is an indication of the presence of secondary flow structures. The secondary flow velocity vector in the transverse plane with 0.3 span is shown in figure 8

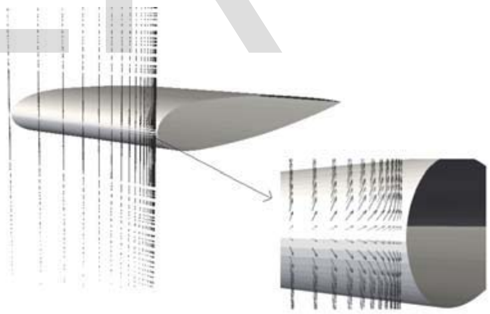

Fig. 8. The secondary velocity in a plane transverse to main flow

The figure 9 shows the contours of secondary kinetic energy for the case with span height of 0.3 times the chord. The red region shows the region with maximum secondary kinetic energy and is the region to be considered for further studies.

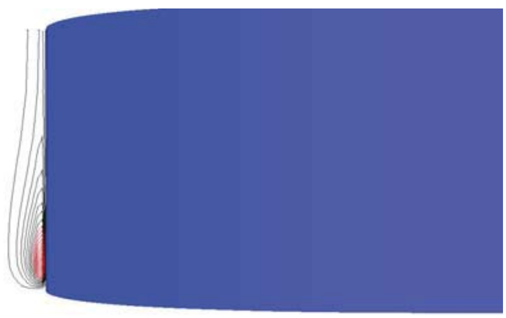

Fig. 9. The SKE contours at leading edge

VIII. Conclusion

The characteristics of flow in axial turbine stator cascade is predicted numerically using an open source CFD tool, OpenFOAM. The following are evident from the analysis

1) The code is validated using the problem of laminar flow over an isolated NACA 0012 aerofoil.
2) The analysis has predicted the secondary flow in the blade passage.
3) The maximum value of secondary flow velocity is found to increase with increase of span for the same value of chord and inlet velocity.
4) The maximum value of secondary kinetic energy occurs at the leading edge near to the endwall.
5) The study provides data for improving the geometry for reducing secondary flow velocity.

References

[1] L. Langston, "Crossflows in a turbine cascade passage," in *American Society of Mechanical Engineers, Gas Turbine Conference and Products Show, New Orleans, La*, 1980.

[2] O. Sharma and T. Butler, "Predictions of endwall losses and secondary flows in axial flow turbine cascades," *Journal of turbomachinery*, vol. 109, no. 2, pp. 229–236, 1987.

[3] C. Sieverding, "Recent progress in the understanding of basic aspects of secondary flows in turbine blade passages," *Journal of Engineering for Gas Turbines and Power*, vol. 107, p. 248, 1985.

[4] H.-P. Wang, S. J. Olson, R. J. Goldstein, and E. R. Eckert, "Flow visualization in a linear turbine cascade of high performance turbine blades," *Journal of turbomachinery*, vol. 119, no. CONF-950629–, 1997.

[5] W. A. Eckerle and L. Langston, "Horseshoe vortex formation around a cylinder," *Journal of turbomachinery*, vol. 109, no. 2, pp. 278–285, 1987.

[6] K. N. Kumar and M. Govardhan, "Secondary flow loss reduction in a turbine cascade with a linearly varied height streamwise endwall fence," *International Journal of Rotating Machinery*, vol. 2011, 2011.

[7] R. Swanson and E. Turkel, "Artificial dissipation mid central differfnce schemes for the euler and navier-stokes equations," 1987.

[8] S. Lal, "A numerical investigation of rotor-stator interaction in turbine stage," *PhD Thesis*, vol. 1, no. 1, pp. 168–172, 2001.

[9] G. Zess and K. Thole, "Computational design and experimental evaluation of using a leading edge fillet on a gas turbine vane," *Transactions of the ASME-T-Journal of Turbomachinery*, vol. 124, no. 2, pp. 167–175, 2002.